Experimental/numerical characterization of hygrothermal ageing in glass/epoxy composites

Barcelos Carneiro M Rocha, Iuri; Raijmaekers, S; Nijssen, RPL; van der Meer, Frans; Sluijs, Bert

Publication date
2016

Document Version
Final published version

Published in
Proceedings of the 17th European Conference on Composite Materials

Citation (APA)
Barcelos Carneiro M Rocha, I., Raijmaekers, S., Nijssen, RPL., van der Meer, F., & Sluijs, B. (2016). Experimental/numerical characterization of hygrothermal ageing in glass/epoxy composites. In K. Drechsler (Ed.), *Proceedings of the 17th European Conference on Composite Materials: Munich, Germany* (pp. 1-8). KIT.

EXPERIMENTAL/NUMERICAL CHARACTERIZATION OF HYGROTHERMAL AGEING IN GLASS/EPOXY COMPOSITES

I.B.C.M. Rocha[1,2], S. Raijmaekers[1], R.P.L. Nijssen[1], F.P. van der Meer[2], L.J. Sluys[2]

[1]Knowledge Centre WMC, Kluisgat 5, 1771MV Wieringerwerf, The Netherlands
[2]Delft University of Technology, P.O. Box 5048, 2600GA Delft, The Netherlands

Keywords: Hygrothermal ageing, Glass/Epoxy composites, Material degradation, Multiphysics analysis, Concurrent (FE^2) homogenization

Abstract
In this work, a combined experimental/numerical approach is used to investigate the effect of water ingression in glass/epoxy composite specimens. Interlaminar shear (ILS) specimens were immersed at 50°C for multiple durations and tested. Re-dried specimens were also tested. Significant strength degradation of up to 50% was found for wet specimens, while dried ones showed an irreversible decrease in strength of approximately 9%. The diffusion phenomenon was also investigated numerically in a multiscale/multiphysics framework. At the microscale, an RVE combining linear-elastic fibres, elasto-plastic resin with damage and cohesive interfaces was used. At the macroscale, a classic stress equilibrium analysis is coupled with a Fickian diffusion model, and an independent micromodel is run at each macroscopic integration point. The model was used to simulate diffusion in a short-beam specimen and regions of plastic deformation, interface failures and softening bands in the resin were identified.

1. Introduction

Research on composite material usage optimization for wind turbine blades has been on the rise in the past few years, and particular focus is being given to reducing design uncertainty through a better understanding of material interaction with extreme service environments. Among many types of environmental attack, the combined influence of temperature and moisture ingression is regarded as the most critical one [1]. Upon exposure to humid environments, polymers tend to absorb water molecules through a diffusion process driven by pressure gradients. Once inside, water tends to plasticize the resin and cause swelling, as well as chemically break polymer chains

Experimental observations in a glass/epoxy system used in wind turbine blades suggest that diffusion mechanics and material degradation tend to be well predictable for short duration exposure of neat resin specimens, while for composites the presence of fibres brings differential swelling stresses which do not vanish upon saturation [2]. Furthermore, when conditioned at high temperatures and for extended durations, water can chemically attack the fibres and their sizing [3],

This work seeks to characterize degradation processes in unidirectional glass/epoxy specimens after water immersion at 50°C. In order to evaluate the combined effect of interface and matrix damage, ILS specimens were chosen. Mechanical tests are performed and the evolution of material properties with immersion time is obtained. The ageing process is also investigated through modelling using FEM in a multiscale environment. At the microscopic level, a 2D Representative Volume Element (RVE) with random periodic fibre distribution is considered, and cohesive-zone elements are used around every fibre

Excerpt from ISBN 978-3-00-053387-7

in order to capture interfacial failure. The micromodel includes mechanical strains with periodic boundary conditions, as well as swelling strains in the resin. Such model is embedded in an FE^2 framework where the averaged deformation is prescribed from a macroscopic model, which in turn receives stiffness and stress from the micromodels at each material point. In order to capture transient swelling strains, water diffusion is also modelled in the macroscale, and the water concentration field is passed to the micromodels at every time step. Results obtained from such diffusion analysis are qualitatively compared with experimental ones, considering both mechanical performance and observed fracture surfaces after immersion.

2. Experiments

2.1. Materials and Methods

The glass/epoxy material considered in this work is a combination of the EPIKOTE RIMR 135/EPIKURE RIMH 1366 epoxy resin with unidirectional glass fibre fabrics composed of PPG Hybon 2002 glass fibre rovings. Originally, the UD fabric includes a stability roving layer oriented at 90°, making up for 5% of the fabric in weight. However, in order to reduce complexity in the material behaviour and simplify the modelling effort, such layer was manually removed, resulting in a strictly UD fabric. A 3-ply 320x320x2.15mm^3 panel was manufactured through vacuum infusion molding (Figure 1a) and was cured for 2h at 30°C, 5h at 50°C and 10 h at 70°C. ILS short-beams with nominal dimensions 21.5x10.75x2.15mm^3, in accordance with the ISO 14130 standard, were cut from the panel using a CNC milling machine.

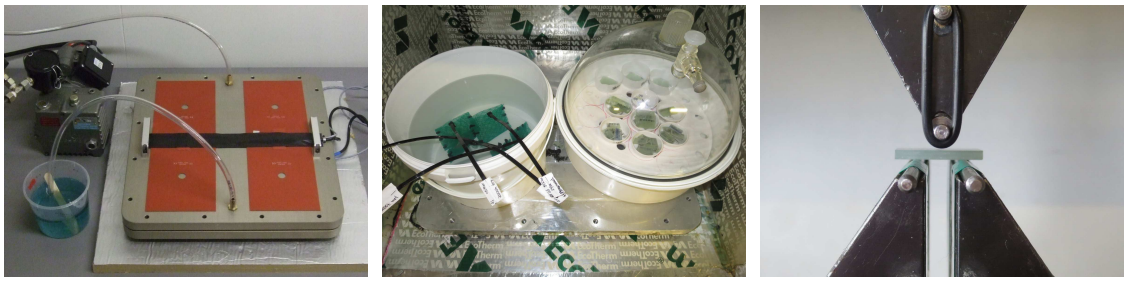

(a) Manufacturing (b) Conditioning (c) Testing

Figure 1: Experimental programme workflow.

After manufacturing, a set of specimens was kept as reference and the rest was immersed in demineralised water at 50°C for multiple durations. In order to investigate the material degradation due to water ingression in a consistent way, it is important that the specimens chosen as reference (unaged) are moisture-free. Also, as mechanical tests will be performed on specimens dried after being immersed, it is important to account for ageing processes that may occur during this drying step. Therefore, all specimens were first dried for 1200 h in a silica gel desiccator at 50°C and periodically weighed in order to guarantee a moisture-free state. In order to speed up the drying and avoid oxidative reactions, vacuum was periodically reapplied to the desiccator. The same setup was also used to dry specimens which were previously immersed. The immersion and drying setups can be seen in Figure 1b.

After conditioning, sets of 10 specimens were quasi-statically tested in three-point bending in an MTS test frame with a 10kN load cell. The span was fixed at 11.4mm and steel cylinders of 3.14mm and 6mm diameter were used as supports and loading nose, respectively (Figure 1c). The tests were conducted at a rate of 1mm/min until a displacement of 0.9mm was reached, a point when reference specimens have already suffered significant load drops and secondary failure modes (tension, compression) start to occur. The maximum attained load is recorded and the interlaminar shear strength (ILSS) is calculated as

Excerpt from ISBN 978-3-00-053387-7

$0.75 \cdot F_{max}/area$. Sets were tested wet after 250 h, 500 h, 1000 h, 1500 h and 2000 h and dry after being immersed for 500 h and 1000 h.

2.2. Results and Discussion

Results from the performed mechanical tests can be seen in Figure 2 and Table 1. To avoid clutter, only one representative curve for each series of 10 specimens is shown in Figure 2a, while the evolution of average and standard deviation values with immersion time can be seen in Figure 2b, where results from dry tests are shown as circle markers. In order to relate the incurred degradation with the water mass inside the specimens, the water uptake evolution in time is also shown in Figure 2b.

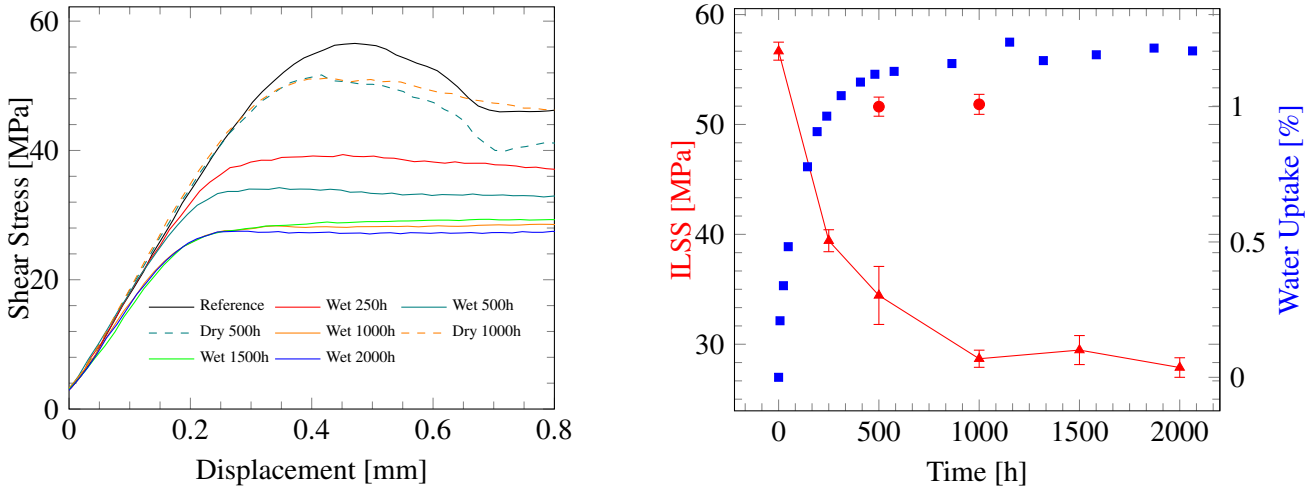

(a) Stress-displacement curves.

(b) Strength and water uptake evolution.

Figure 2: ILSS test results after immersion.

From results of specimens tested wet, it can be seen that the strength gradually decreases with immersion time from approximately 57 MPa, at first with a higher rate, while reaching a stable value of around 29 MPa after 1000 h, a decrease of around 50%. Comparing such evolution with the water uptake measurements, an approximately linear relationship between uptake and strength can be observed. While previous experiments [4] suggest that time-dependent degradation and uptake mechanisms exist for this material system, they were not significant for the shorter durations considered in this work.

	Reference	250h	500h	1000h	1500h	2000h
Tested wet						
$\tau_{\max}$ [MPa]	-	39.4 ± 1.0	34.4 ± 2.6	28.7 ± 0.9	29.5 ± 1.3	27.9 ± 0.9
Tested dry						
$\tau_{\max}$ [MPa]	56.7 ± 0.8	-	51.6 ± 0.9	51.8 ± 0.9	-	-

Table 1: ILSS values for short-beam specimens.

On the other hand, results from specimens dried after being immersed suggest that the degradation does not depend only on the current uptake, as an irreversible strength reduction was observed. Furthermore, this irreversible degradation does not seem to depend on time, as results are similar for both 500 h and 1000 h specimens. It is thus hypothesised that such behaviour is the result of material failure due to differential swelling stresses developed during the diffusion process.

Excerpt from ISBN 978-3-00-053387-7

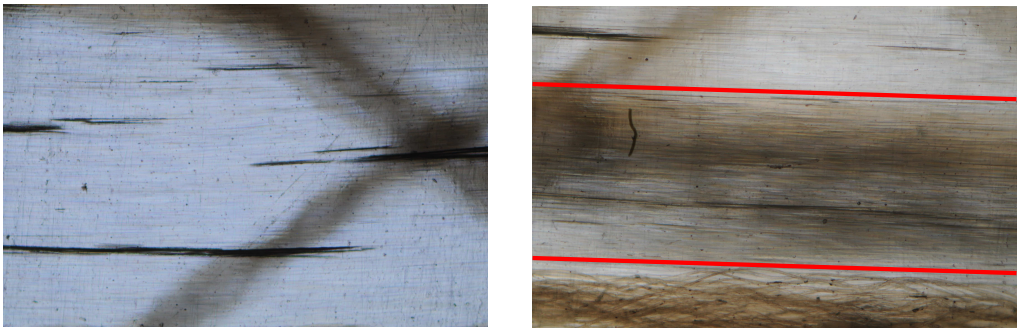

(a) After 250h (b) After 2000h

Figure 3: Microscopic observations of interface cracking (4x magnification).

Lastly, specimens were inspected in an optical microscope after having been immersed for 250 h (Figure 3a) and 2000 h (Figure 3b). Both pictures were taken in the $x - y$ plane with 0° fibres oriented horizontally (plies are stacked along the z axis). It can be seen that cracks along the fibre-matrix interface can be observed even after only 250 h of immersion (stitches are seen as diagonal bands in the first picture and as horizontal strands at the bottom of the second picture). The cracks are initially concentrated close to the surface and in a small number of fibres, but crack bands as the one delimited by the red lines in Figure 3b start to develop after approximately 1300 h of immersion. As the specimens were already saturated at this point, such behaviour points to the existence of a time-dependent weakening of the interface, even though its impact on the measured interfacial strength was not significant up until 2000 h of immersion.

3. Modelling

3.1. RVE Model

Since water affects each material component (fibre, matrix, interface) differently and numerical evidence suggests that differential swelling stresses can be significant in regions where fibres are closely packed [2], a micromechanical modelling approach is adopted in this work. The micromodel consists in a 2D Representative Volume Element (RVE) of unidirectional fibres and surrounding matrix, with the main fibre direction oriented out of the plane. Geometrically periodic RVEs with an arbitrary number of randomly distributed fibres are generated by the discrete element package HADES. A mesh of triangular finite elements is generated using Gmsh and 2D interface elements are generated around every fibre at runtime. The swelling of the resin is modelled as an applied strain at every integration point and depends linearly on the water concentration at the point.

In order to correctly describe material failure during immersion, suitable constitutive models have to be chosen for each material component. Here, the fibres are modelled as linear-elastic and their failure is not considered. Cracking along the fibre-matrix interface is modelled using the mixed-mode Cohesive Zone traction-separation law formulated by Turon et al [5], consisting of an initially stiff linear part followed by linear softening when the fracture strength is reached. For the numerical examples in the present work, interface strength and fracture toughness values obtained by Li [6] through fibre pushout tests were used.

The epoxy resin is modelled as elasto-plastic with damage, using the model formulated by Melro et al [7]. The model is composed of a linear-elastic portion followed by plastic hardening and transitioning to damage with exponential softening after the fracture strength is reached. The model was calibrated

Excerpt from ISBN 978-3-00-053387-7

using results from uniaxial tension and compression tests, resulting in the hardening curves shown in Figure 4a. A comparison between numerical and experimental stress-strain behaviour can be seen in the red and blue curves of Figure 4b, where the model is shown to correctly represent the material in both tension and compression.

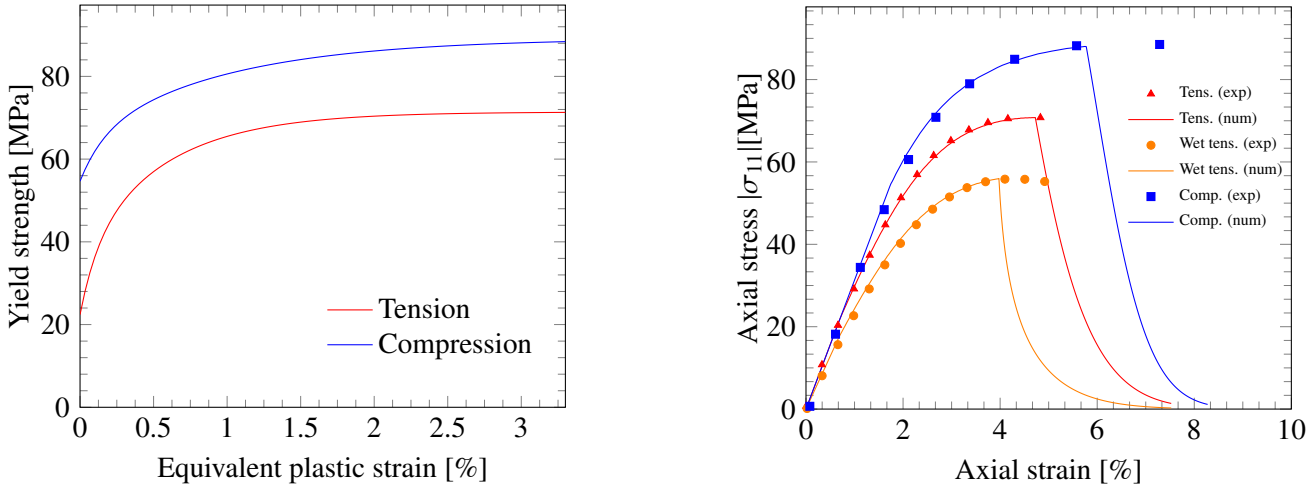

(a) Input hardening data.

(b) Validation with experimental results.

Figure 4: Calibration of the elasto-plastic model with damage for epoxy.

Lastly, material properties were also made to be a function of water concentration. Previous experimental results [4] show that the mechanical behaviour of neat resin changes after water absorption, with up to 20% lower modulus and fracture strength at saturation. This effect is modelled here by considering that both stiffness, yield stress and strength show a linear decay with water concentration. Furthermore, it is assumed that all properties show the same decay ratio. In order to assess the validity of such hypothesis, the properties used to obtain the dry curve shown in red on Figure 4b were knocked down by 20% in order to obtain the orange curve, which showed good agreement with the curve obtained experimentally using a saturated specimen.

3.2. Multiscale Analysis

The micromodel described in the previous section can be used to predict material degradation by prescribing the water concentration of every resin node and solving the non-linear equilibrium problem. In order to make the model representative of a macroscopic material point, periodic boundary conditions can be applied while letting the RVE swell freely (zero macroscopic strain). In reality, however, transient macroscopic swelling stresses occur during diffusion due to water concentration gradients [8]. Even though such transient stresses vanish upon saturation, they can make the microscopic stress state more complex and influence material failure at early immersion times.

In order to account for such transient macroscopic stresses, the proposed micromodel is coupled to a macromodel in an FE^2 (Computational Homogenization) approach by associating a micromodel with unique material history to each macroscopic integration point. At the macroscale, a Fickian diffusion model is combined with a mechanical equilibrium model in a multiphysics approach. At each time step, the concentration and strain fields are computed and passed to the micromodels, with strains being applied as boundary conditions and concentration being prescribed to every resin node. The micro boundary-value problem is then solved and homogenised stresses and stiffness values are brought back to the macroscale. The process is then repeated until macroscopic equilibrium is reached.

Excerpt from ISBN 978-3-00-053387-7

In applying the proposed formulation, it is important to choose a suitable RVE size so that the homogenised stiffness and material failure behaviour do not change considerably if the size is further increased. Figure 5 shows changes in the first term of the homogenised stiffness matrix $\overline{D}$ as the water concentration and RVE size are changed.

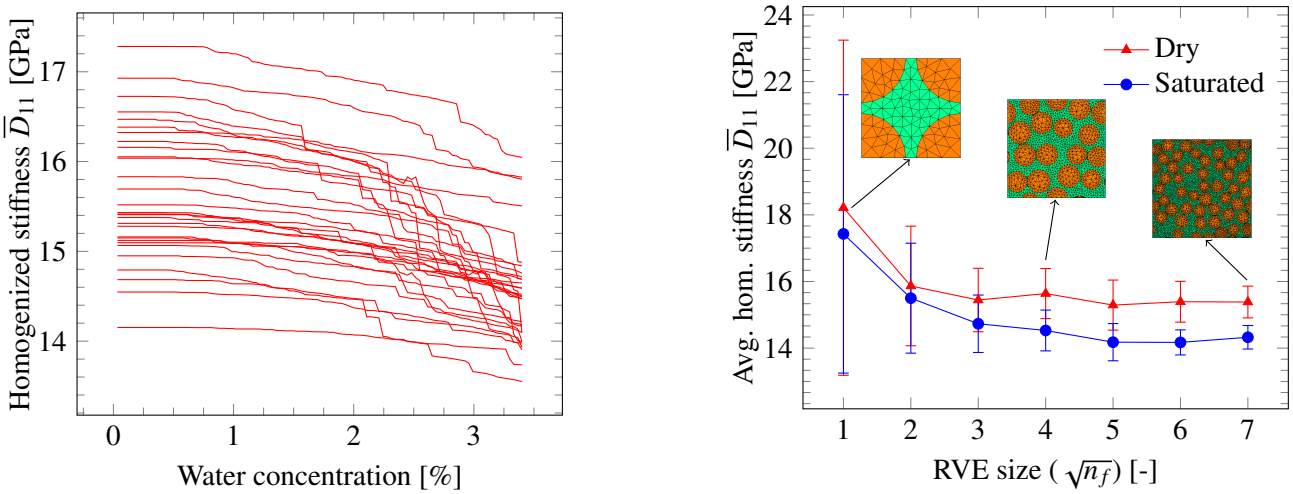

(a) Individual executions of 30 16-fibre RVEs.

(b) Stiffness changes with RVE size.

Figure 5: Effect of RVE size on the homogenised macroscopic stiffness.

As expected, stiffness drops are observed with increased concentration due to matrix hardening and both matrix and interface softening processes, although the scatter for both dry and saturated stiffness can be high, particularly for smaller RVE sizes. Figure 5b shows average and standard deviation values for sets of 30 RVEs with a number of fibres ranging from 1 to 49. As expected, both dry and saturated stiffness values tend to stabilise with an increase in the number of fibres, while the standard deviation tends to decrease. In order to strike a reasonable balance between analysis fidelity and required computational effort, a 25-fibre RVE is used in the example that follows.

3.3. Numerical Example

In order to demonstrate the capabilities of the proposed model, the simulation of the immersion process of an ILSS short-beam is showed. The macromodel is a 2D representation of the specimen along its longitudinal axis, with diffusion along the length being ignored for the sake of simplicity. The immersion is simulated by prescribing constant water concentration at all boundaries while letting the specimen swell freely in both x and y directions. The transient problem is then run from $t = 0$ h to $t = 600$ h with a time step of 10 h.

Figure 6 shows the evolution of RVE displacements due to swelling as well as of the occurrence of material failure for a point close to the bottom surface of the specimen at mid-width. At first, the point experiences no swelling since the initial concentration is set to zero (Figure 6a). At $t = 40$ h, the point is already very close to saturation, but cannot swell freely in both x and y directions since transient macroscopic stresses compress the RVE in the x direction. This additional constraint creates a softening band in the resin at the point marked with a red circle in Figure 6b, which does not occur at other points in the specimen. Interface failures can also be seen at the points marked with orange circles, while the coloured resin bands represent plastic zones. Finally, at $t = 600$ h, the transient stresses vanish due to macroscopic saturation and the RVE has finished swelling. It is important to note that, even though the macroscopic swelling stresses vanish, microscopic differential swelling persists even after saturation.

Excerpt from ISBN 978-3-00-053387-7

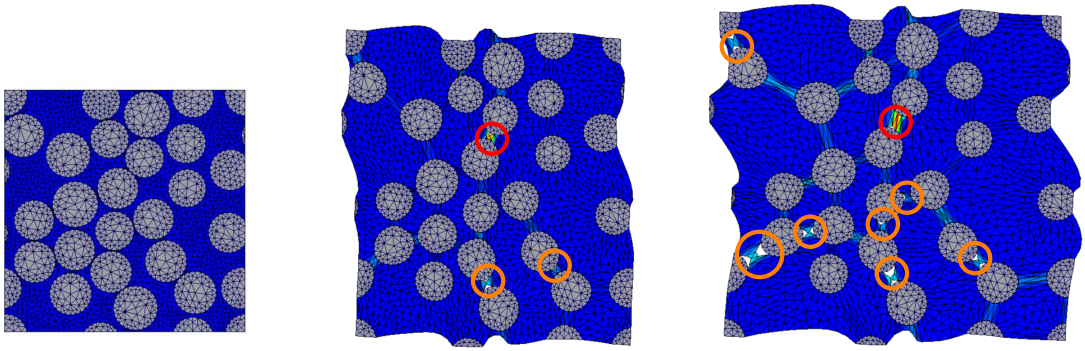

(a) t = 0 h (b) t = 40 h (c) t = 600 h

Figure 6: Microscopic state evolution for a material point close to the surface

Results from the present numerical simulation suggest that the impact of water on the mechanical properties of composite samples is composed of three parts. Firstly, differential swelling stresses which persist even after saturation and create a state of initial stresses that impact the perceived strength measured through mechanical tests, secondly, degradation of stiffness and strength due to phenomena such as plasticization and thirdly, plasticity and cracking caused by a combination of differential swelling and transient macroscopic swelling stresses. While the first two effects will vanish if the specimen is dried back to a moisture-free state, the third one is irreversible, which would explain the observed residual degradation in specimens tested dry after having been immersed for 500 h and 1000 h (Section 2.2).

4. Conclusions

In this work, the effects of water ingression in the mechanical properties of glass/epoxy specimens was assessed by combining results from mechanical tests to qualitative results obtained using a multiscale/multiphysics numerical model.

Interlaminar shear (ILS) specimens were tested after having been immersed for multiple durations, including specimens dried before being tested. For wet specimens, the measured strength suffered decreases of up to 50% after immersion when compared to reference values, while dried specimens showed an irreversible reduction of approximately 9%. Inspection in an optical microscope showed crack formation along the fibre-matrix interface after immersion for a period as short as 250 h, while bands of cracks started to appear after approximately 1300 h of immersion.

In order to numerically simulate water diffusion and swelling, a multiscale FE^2 approach was used. The 2D micromodel combines a linear-elastic model for the fibres, an elasto-plastic model with damage for the resin and a cohesive traction-separation law for the interface. At the macroscale, a multiphysics model combining stresses and diffusion is used, and each integration point is linked to a micromodel with unique material history. The obtained numerical results showed the occurrence of interface and resin softening and the formation of plasticity bands during diffusion.

Besides providing additional insight on the material behaviour during immersion, the potential of the proposed numerical model can be further extended by applying static or fatigue mechanical loads and investigating the propagation of the newly-created cracks.

Excerpt from ISBN 978-3-00-053387-7

Acknowledgments

The authors acknowledge the contribution of the TKI-WoZ and IRPWIND projects and partners for motivating and partly funding this research.

References

[1] J. R. White and T. A. Turnbull. Review: Weathering of polymers: mechanisms of degradation and stabilization, test strategies and modelling. *Journal of Materials Science*, 29:584–613, 1994.

[2] Y. Joliff, W. Rekik, L. Belec, and J. F. Chailan. Study of the moisture/stress effects on glass fibre/epoxy composite and the impact of the interphase area. *Composite Structures*, 108:876–885, 2014.

[3] A. S. Maxwell, W. R. Broughton, G. Dean, and G. D. Sims. Review of accelerated ageing methods and lifetime prediction techniques for polymeric materials. Technical report, National Physical Laboratory (NPL), 2005.

[4] I. B. C. M. Rocha, S. Raijmaekers, R. P. L. Nijssen, and F. van der Meer. Hydrothermal ageing of glass/epoxy composites for wind turbine blades. In *20th International Conference on Composite Materials*, 2015.

[5] A. Turon, P. P. Camanho, J. Costa, and C. G. Dávila. A damage model for the simulation of delamination in advanced composites under variable-mode loading. *Mechanics of Materials*, 38:1072–1089, 2006.

[6] M. Li. *Temperature and moisture effects on composite materials for wind turbine blades*. MSc thesis, Montana State University-Bozeman, 2000.

[7] A. R. Melro, P. P. Camanho, F. M. Andrade Pires, and S. T. Pinho. Micromechanical analysis of polymer composites reinforced by unidirectional fibres: Part I - Constitutive modelling. *International Journal of Solids and Structures*, 50:1897–1905, 2013.

[8] G. Pitarresi, M. Scafidi, S. Alessi, M. Di Filippo, C. Billaud, and G. Spadaro. Absorption kinetics and swelling stresses in hydrothermally aged epoxies investigated by photoelastic image analysis. *Polymer Degradation and Stability*, 111:55–63, 2015.

Excerpt from ISBN 978-3-00-053387-7